AAPS PharmSciTech (2020) 21:251
DOI: 10.1208/s12249-020-01794-x

Check for updates

Research Article

Interfacial Stress and Container Failure During Freezing of Bulk Protein Solutions Can Be Prevented by Local Heating

Andreia Duarte,[1] Pedro Rego,[1] Aida Ferreira,[2] Paulo Dias,[2] Vítor Geraldes,[3] and Miguel A. Rodrigues[4,5]

Received 30 January 2020; accepted 18 August 2020

Abstract. Bottles and carboys are used for frozen storage and transport of biopharmaceutical formulations under a wide range of conditions. The quality of freezing and thawing in these systems has been questioned due to the formation of heterogeneous ice structures and deformation of containers. This work shows that during freezing of bulk protein solutions, the liquid at the air–liquid interface freezes first, forming an ice crust and enclosing the liquid phase. As the enclosed liquid freezes, internal pressure rises, pushing the liquid phase through the porous ice crust towards the air interface, leading to interfacial stress and protein aggregation. The aggregation of bovine serum albumin was more intense in the foam-like ice mound that was formed at the top, where bubbles were entrapped. This was characterized experimentally with the assistance of magnetic resonance imaging (MRI). An isothermal cover is proposed to prevent the early freezing of the liquid at the air interface, attenuating substantially interfacial stress to proteins and releasing hydrostatic pressure, preserving the shape and integrity of the containers.

KEY WORDS: freezing; ice crust; interfacial stress; isothermal cover; pressure increase.

INTRODUCTION

Biopharmaceutical solutions are produced industrially in large batches that are stored for management flexibility. In many cases, the biopharmaceutical solutions are frozen to increase the shelf life of the product and facilitate its transport (1). Usually, the batches are split into smaller volumes to fit inside bottles, carboys, or bags for storing, transporting, freezing, and thawing (2). However, this may require multiple disposable containers, and consequently, multiple container–closures are involved, leading to some risk of contamination (3,4). Although the disposable bags offer some advantages, the potential break of a bag or tubing assemblies, leading to contamination and loss of product, is a serious concern, compared with bottles/carboys (2). In particular, damage of bags during freezing and handling at low temperature is regularly reported (5,6), *e.g.*, during transportation. The bottle/carboy systems are simple and the preferred mode of operation of many companies, especially when biopharmaceutical formulations are robust and stable under a wide range of freeze–thaw conditions (3,4). Notwithstanding, freezing, handling, and transportation of bottle/carboys at low temperature also present risks. Freezing is typically slower and less controlled, and hydrostatic pressure can build up causing the bottles to deform or rupture (6). Some of these adversities are associated with the cooling of the liquid phase at the air–liquid interface, which causes the top of the liquid to freeze first, forming an ice crust, enclosing the remaining liquid phase (6,7). As the enclosed liquid freezes, the liquid phase is pushed through the ice crust towards the air interface, creating an ice mound (7,8). It has been shown that this ice mound is almost pure ice and rich in entrapped air bubbles, and therefore, it is a region of high interfacial stress for proteins, which has been correlated with higher aggregation of monoclonal antibodies (7).

In this work, we evaluate whether installing a top cover on the bottles (insulation with or without a phase-change material) can prevent early freezing of the liquid at the air interface. This is expected to minimize the formation of the

[1] SmartFreeZ, Ed. Inovação II, Incubadora Taguspark, Porto Salvo, Portugal.
[2] Instituto Politécnico de Lisboa, Escola Superior de Tecnologia da Saúde de Lisboa (ESTeSL), Lisbon, Portugal.
[3] CeFEMA, Instituto Superior Técnico, Universidade de Lisboa, Lisbon, Portugal.
[4] CQE, Instituto Superior Técnico, Universidade de Lisboa, Av. Rovisco Pais-1, 1049-001, Lisbon, Portugal.
[5] To whom correspondence should be addressed. (e–mail: miguelrodrigues@tecnico.ulisboa.pt)

aaps
Published online: 01 September 2020

ice mound at the top, preventing deformation of the container due to pressure, while attenuating interfacial stresses and potentially ameliorating protein stability.

MATERIALS AND METHODS

Protein Solution

A bovine serum albumin (BSA) solution at 1% (w/v) with 5% (w/v) sucrose and 0.3% (w/v) sodium chloride was used as a model protein solution for this study. All the reagents were purchased from Sigma-Aldrich. BSA was selected for this study because it is a medium-sized protein (66 kD) that is very well studied and characterized.

Containers

Bottles of 2 L and 5 L (model PharmaTainer), made of polyethylene terephthalate (PET) with a wall thickness of 2 mm, were supplied by Cellon (Luxembourg). The 5-L PET bottle with thinner walls (thickness of 1.2 mm) was supplied by LaborSpirit (Portugal). Bottles with 2 L of volume were used for all the studies, since they are commonly used in the pharmaceutical industry and are easier to handle and to sample (with a bench-top band saw). Bottles with 5 L of volume were also used for the pressure deformation studies, as square bottles of different wall thicknesses were readily available in this size.

Insulation of the Bottle Head Space

The head space region of the bottles was insulated with covers made of a material with low thermal conductivity, to attenuate cooling of the air inside the bottle's head space during freezing. Two covers were used (Fig. 1): an isothermal cover with an internal cavity filled with water (300 mL) to act as a phase-change material (PCM) and an insulating cover without PCM. The covers were produced by additive manufacturing (3D printed) in a Ultimaker 2+ (Ultimaker, Netherlands) using polylactic acid (PLA, SMARTFIL® PLA, ref. SMPLA0WH0A075). The shape of the covers was adjusted to snuggly fit to the head space of the bottle. The covers were configured to assure that the quantity of PCM was not higher than 20% of the volume of the solution to freeze and this quantity of PCM was calculated for the external wall thickness used (10 mm) and type of material (PLA), on the total area to insulate and external heat transfer coefficient.

Freezing and Pressure Analysis

The pressure inside the bottles during freezing was measured using a thin film pressure transducer (PX603-5KG5V, Omega). The 5-L bottles were frozen without any cover, while the 2-L bottles were frozen with and without the isothermal cover with PCM. The pressure transducer was placed in the center and middle of the bottles, preferentially in the last point to freeze (Fig. 2). The 5-L bottles were filled with 4.8 L of protein solution and the 2-L bottle with 1.8 L. Then, the bottles were frozen inside a wind tunnel with a vertical (unidirectional) flow of gas with average ascending velocity of 3.5 m/s and -75 ± 2°C (Fig. 3). The average velocity was measured with a hot-wire anemometer (Testo 405i, Testo, USA). The pressure transducer was calibrated for the atmospheric pressure, and the effect of temperature on the pressure transducer was evaluated. No significant effect of temperature on the pressure signal was observed in the range between 20 and −50°C.

Freezing and Ice Macro-structure Analysis

To visualize how the ice grows inside the bottles, a 2-L bottle was cut in half by the central vertical plane, and each half was sealed to a 2-mm transparent acrylic plate with silicone glue. The 2-L bottle was reconstituted by joining (and compressing) the two acrylic plates with rubber bands, ensuring a negligible air gap between the plates, as shown in Fig. 4. With this configuration, it was possible to freeze in the same setup and under the same conditions two bottles with different covers, also allowing to observe the ice front progression inside the bottles during the freezing process. Two assays were performed: in the first, one of the halves of the bottle was covered with the insulating cover without PCM, while the other was kept without any cover; in the second, one of the halves of the bottle was covered with the isothermal cover with PCM, while the other was kept without a cover. Each half of the bottle was filled with 0.9 L of protein solution and the bottom of the bottle placed on top of extruded polystyrene support, to keep it insulated. The bottle was frozen inside the low-temperature chamber at −75°C. After the freezing process, the bottles were stored at −80°C. To sample the frozen solution, the halves of the bottle were separated from the acrylic plate and the surface was warmed with tap water for a slight thaw at the walls to loosen and remove the frozen block from the bottle. The frozen blocks were cut into small pieces according to a predetermined template to obtain a detailed map of the protein distribution. A bench-top band saw was used to cut the frozen blocks into approximately $1.7 \times 1.7 \times 1.7$-cm cubes, which were then thawed at room temperature to further analysis. The band saw stage was pre-cooled with "dry ice," and all samples were kept in dry ice, except when they were being cut.

Protein concentration and the percentage of aggregates were measured by size-exclusion high-performance liquid chromatography (SEC-HPLC) (Agilent 1100 system) using a diode array detector (G1315B Agilent) at 280 nm. Before pipetting the samples into the HPLC vials, each sample was centrifuged for 5 min at 10,000 rpm to remove particles. The SEC-HPLC was conducted using BioBasic SEC 300 column (7.8×300 mm, 5 μm, Thermo Scientific) in a 50 mM phosphate buffer with 100 mM NaCl at 1 mL/min, and 10 μL of each sample was injected. The concentration of BSA monomer was determined by the area of the absorbance peak with a retention time of 7.8 min. The total BSA concentration (dissolved) was quantified by integrating also the peaks with lower retention time, which are referent to aggregates. Relative local concentration (C/C_0) was determined as the total BSA concentration measured in the samples (after thawing) (C) divided by the initial concentration (C_0) before freezing. The aggregate percentage was determined by dividing the area of the monomer peak by the total area (including the peaks of heavier molecular weight species).

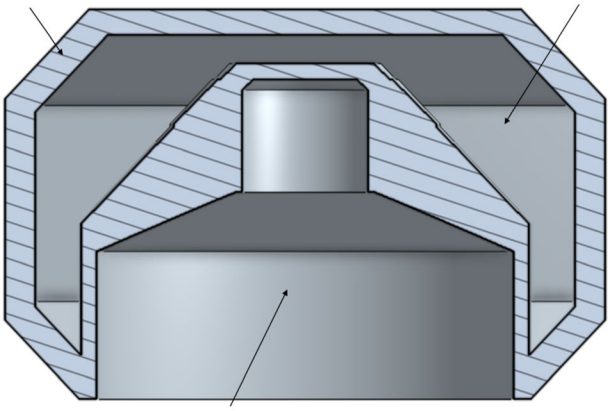

Fig. 1. Schematic representation of the covers used. In the isothermal cover, the internal cavity was filled with PCM (water), while in the insulating cover, the internal cavity was kept without PCM

The map of aggregate distribution shows the increment in the percentage of aggregates after freezing, which is the percentage aggregates in a sample, subtracted by the percentage of aggregates in the initial solution (before freezing).

Freeze–Thaw Assays

Three different freeze–thaw possibilities were evaluated using 2-L bottles: one bottle was frozen and thawed with the isothermal cover, another bottle was frozen and thawed without a cover, and a third bottle was frozen with an isothermal cover and thawed without a cover. Freezing was carried out as previously described, and thawing was carried out inside a chamber with a vertical flow of gas at 6 ± 2°C for 18 h. After thawing, samples of 0.5 mL were collected at different liquid heights, using a syringe connected to a thin tube (with 1/16 in. of diameter). The samples were collected slowly and sequentially from the top of the liquid surface to the bottom, ensuring that the stratification of the solution was not destabilized by the previous sample withdrawal. The total concentration (all solutes) was measured through the refractive index using a refractometer (series 300, Zuzi), and the ratio of local solute concentration relative to initial concentration (C/C_0) was calculated.

Magnetic Resonance Imaging

The frozen bottles were analyzed by magnetic resonance imaging (MRI) in order to clarify the ice growth effect, redistribution of the solutes, and entrapped bubbles. The MRI experiments were performed on a 1.5-T whole-body GE Signa Excite HD MRI scanner (GE Healthcare, Milwaukee, WI, USA) using a quadrature transmit–receive head coil by GE Healthcare and a GE 8 channel CTL cervix, thorax, and lumbar spine coil. The scan protocol included axial and coronal T1-weighted Fast Spin Echo series, 380-mm field of view, 3-mm slice thickness, 0.3-mm interslice gap, repetition time/echo time 425/9.0 ms, bandwidth 31.25 MHz, NEX 2, matrix size of 512/512. The 2-L half bottles were analyzed, one half frozen without insulation and the other half frozen with the isothermal cover containing PCM, as shown in Fig. 4. In order to observe the entrapment of bubbles in the ice structure, the solutions were gently agitated before freezing to ensure the formation of bubbles. The bottles were stored at −80°C for 2 h before the MRI experiments, at which they were placed in a cooler at −10°C. Stabilization above the glass transition temperature of the solution is necessary for enabling mobility of the hydrogen nuclei so that contrast can be observed.

RESULTS

Ice Crust Formation During Freezing

The ice crust was observed and measured in the solution frozen inside the half bottles (with and without a cover). Figure 5 shows that both half bottles developed an ice crust during freezing when the cover was used without PCM, although the insulating cover (without PCM) attenuated the

Fig. 2. Pressure measurement setup for 2-L (left) and 5-L (right) bottles with a pressure transducer placed at the center of the volume of the bottles

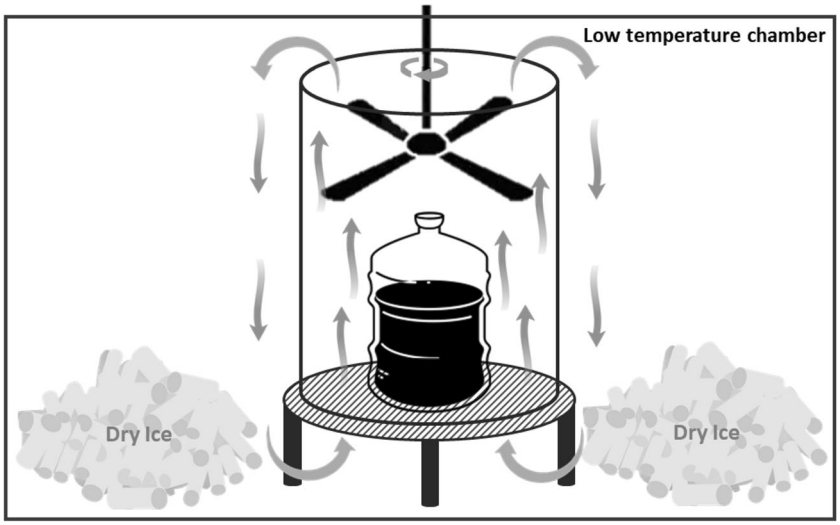

Fig. 3. Schematic depiction of the freezing system. A low-temperature chamber cooled with dry ice. The bottles were placed in a vertical wind tunnel with bottom-up gas flow

ice crust thickness to one-third (1 cm) (Fig. 5b) compared with the uncovered half (3 cm) (Fig. 5a). The ice crust was only fully attenuated in the experiment shown in Fig. 6 when the cover was filled with PCM, *i.e.*, as an isothermal cover. In this case, with the isothermal cover, the liquid was not enclosed by the ice crust and a flat interface was observed (Fig. 6b). Conversely, the half without a cover shows a pronounced "pyramidal" shape crust on the air interface (Fig. 6a).

Hydrostatic Pressure During Freezing

The freezing experiments with a pressure transducer revealed that the hydrostatic pressure in 5-L bottles reached approximately 10 bar (Fig. 7). The bottle with thinner walls (Fig. 8a) deformed substantially, and the bottom became convex releasing the internal pressure (Fig. 7). The bottle with thicker walls reached a pressure plateau at approx. 10 bar (Fig. 7), only slight deformation was observed on the lateral walls (Fig. 8b), and no deformation was observed in the bottom. The internal pressure inside the 2-L bottles did not increase, remaining at atmospheric pressure throughout the freezing process (Fig. 7).

Internal Structure of Frozen Solutions

The MRI enabled to observe the structure of the ice matrix that was formed with and without the isothermal cover. The images in Fig. 9 show dark areas that correspond to the solid (ice) where the hydrogen nuclei have no mobility,

Fig. 4. Two halves of a 2-L bottle glued with silicone to a 2-mm transparent acrylic plate

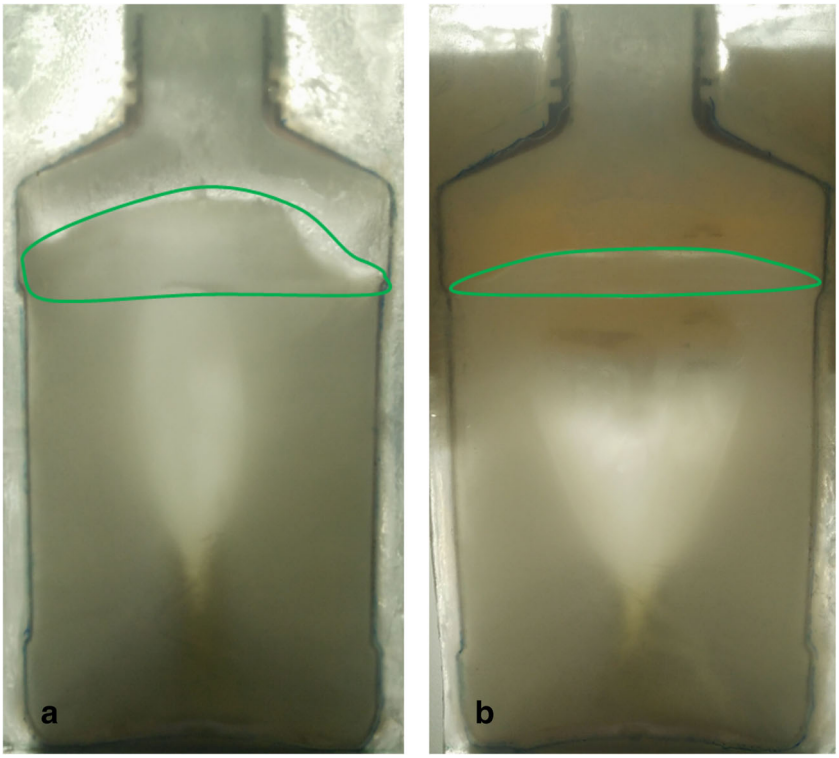

Fig. 5. Ice profile in a 2-L bottle frozen at −75°C for 2 h. Panel **a** presents an uncovered bottle. Panel **b** presents a bottle with the insulating cover without PCM. The ice crust is highlighted by the green circle

whereas white areas correspond to the viscous phase where the hydrogen nuclei have motility (9). The structure of the ice on the top is clearly influenced by the cover (Fig. 9). The bottle without a cover shows a thin layer of highly concentrated solution at the top of the ice mound. This concentrated layer is particularly localized near the walls of the bottle, as

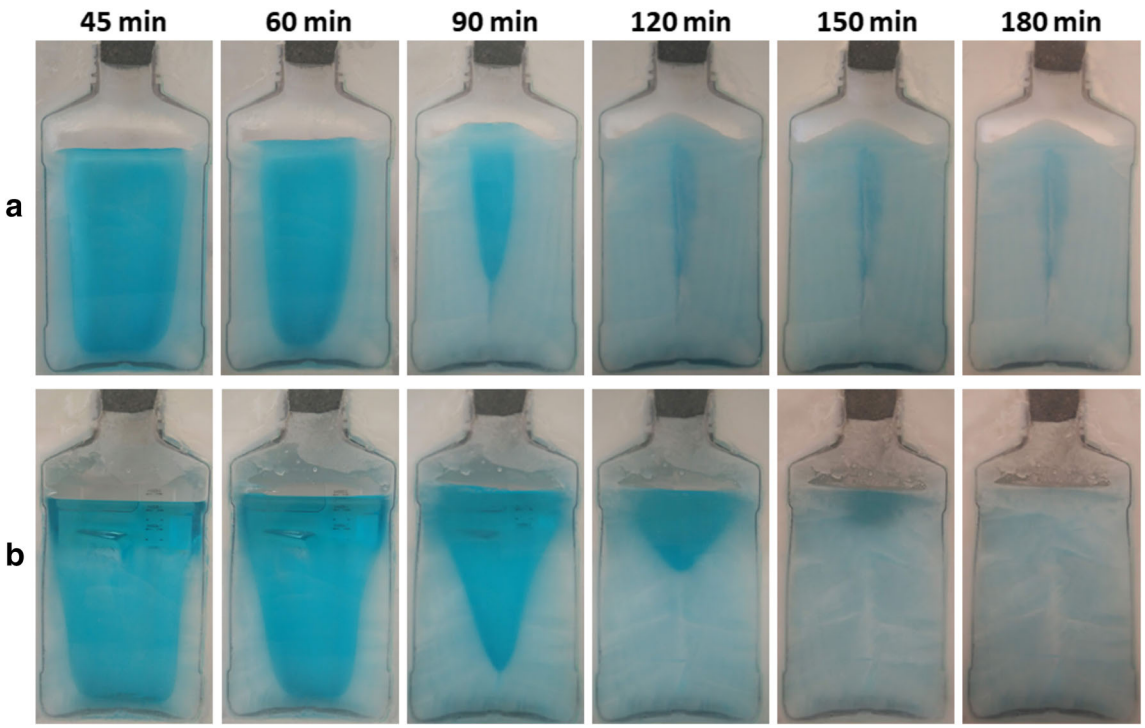

Fig. 6. Ice profile in a 2-L bottle during the freezing process at −75°C for 3 h. Panel **a** presents a bottle without insultation, and panel **b** presents a bottle with the isothermal cover with PCM. To improve the visualization of ice growth, a blue dye was added to the solution

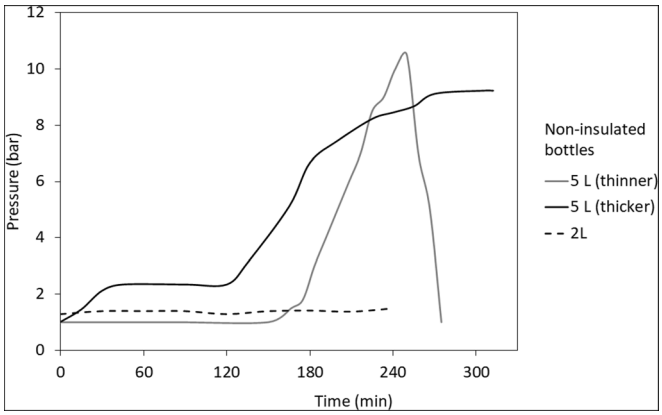

Fig. 7. Pressure rise inside non-insulated bottles. A 5-L bottle with thinner walls (gray line), a 5-L PET bottle (black line), and a 2-L PET bottle (dashed line) during the freezing process at − 75°C

can be observed by the intense white regions indicated by the arrows in Fig. 9a. A more concentrated region is also observed in the center of the bottle, corresponding to the region of the enclosed liquid phase during the freezing process, as previously described. Entrapped bubbles are also evident in the bottle without a cover, as a black layer immediately below of the ice mound. This layer of air partially separates the ice mound from the ice "body" of the bottle. Visually, the ice mound in the top of the uncovered bottle appeared to be more porous (more bubbles per volume) and brittle (during cutting) than the ice in the center of the bottle. The bottle with the isothermal cover (Fig. 9b) shows a more even distribution of the liquid phase, only a thin layer of concentrated solution is observed at the bottom of the bottle. There is also a top differentiated layer, with bubbles, although its volume is 2 times smaller than what is observed in the bottle without a cover.

Protein and Aggregate Distribution During Freezing

The distribution of local concentrations is generally similar in both bottles, with higher concentrations at the center and bottom; however, the uncovered bottle shows an asymmetric top, with a diluted side ($C/C_0 < 1$) and a concentrated side ($C/C_0 > 1$) (Fig. 10). The bottle without a cover shows a generally higher aggregation as illustrated in Fig. 10 (red areas are larger and more intense). Maximum aggregation was spotted in the uncovered bottle at the wall of the "concentrated side" underneath the ice crust, with 10% more aggregates than the initial solution (before freezing).

Solutes Redistribution During Thawing

During thawing, the cover has the reverse effect, cools the top of the bottle, which can have an impact on the final

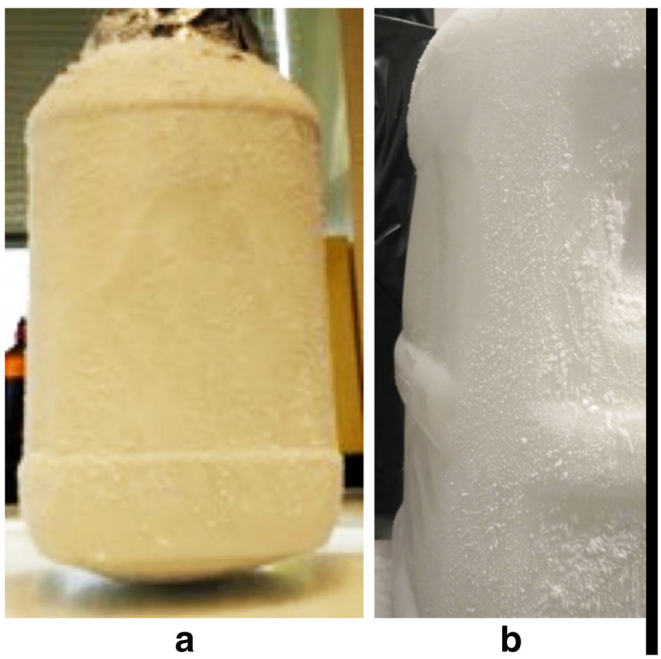

Fig. 8. Panel **a** shows a 5-L bottle with thinner walls, after frozen, with a substantial deformation and a convex bottom. Panel **b** shows a 5-L bottle with thicker walls with a slight deformation in the lateral wall

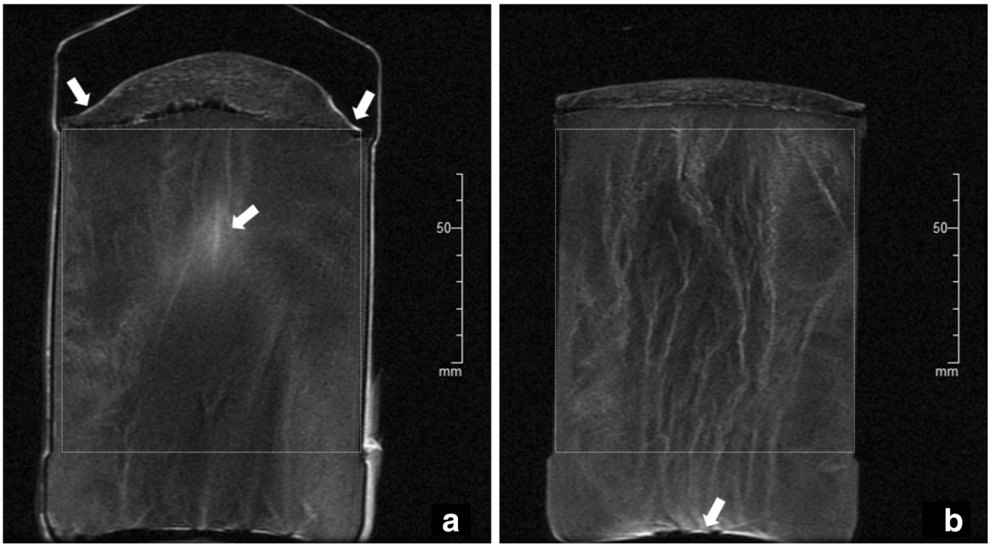

Fig. 9. Internal structures of the frozen solution in a bottle without insulation (**a**) and a bottle with the isothermal cover (**b**). The white arrows indicate the highly concentrated regions

distribution of concentrations. To understand whether thawing is influenced by the different ice structures created by the use of the isothermal cover, or simply by its cooling effect promoted during thawing, three experiments were performed: one bottle was frozen and thawed with an isothermal cover, another bottle was frozen and thawed without a cover, and a third bottle was frozen with an isothermal cover and thawed without the cover. A slow thawing experiment (constant temperature at 6°C) was chosen in order to evaluate the effect of the cover under slow thawing, minimizing convection. As observed in Fig. 11, the solutes were distributed along the bottle, with the top

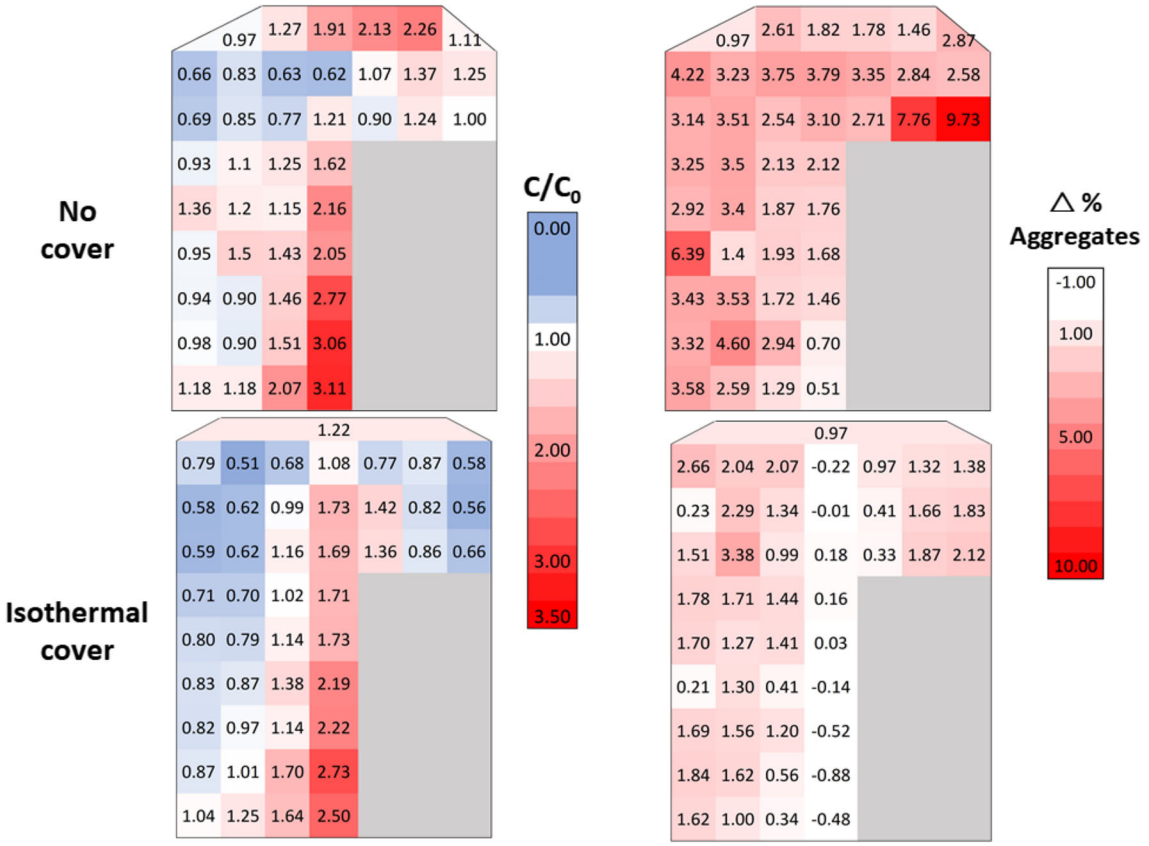

Fig. 10. Distribution of BSA in a 2-L bottle, measured after sampling a frozen solution. On the left is shown the local concentration defined as a cryoconcentration ratio (C/C_0), for bottles frozen with and without an isothermal cover (bottom and top respectively). On the right is shown the corresponding increment in % of aggregated species for bottles frozen with and without an isothermal cover (bottom and top respectively)

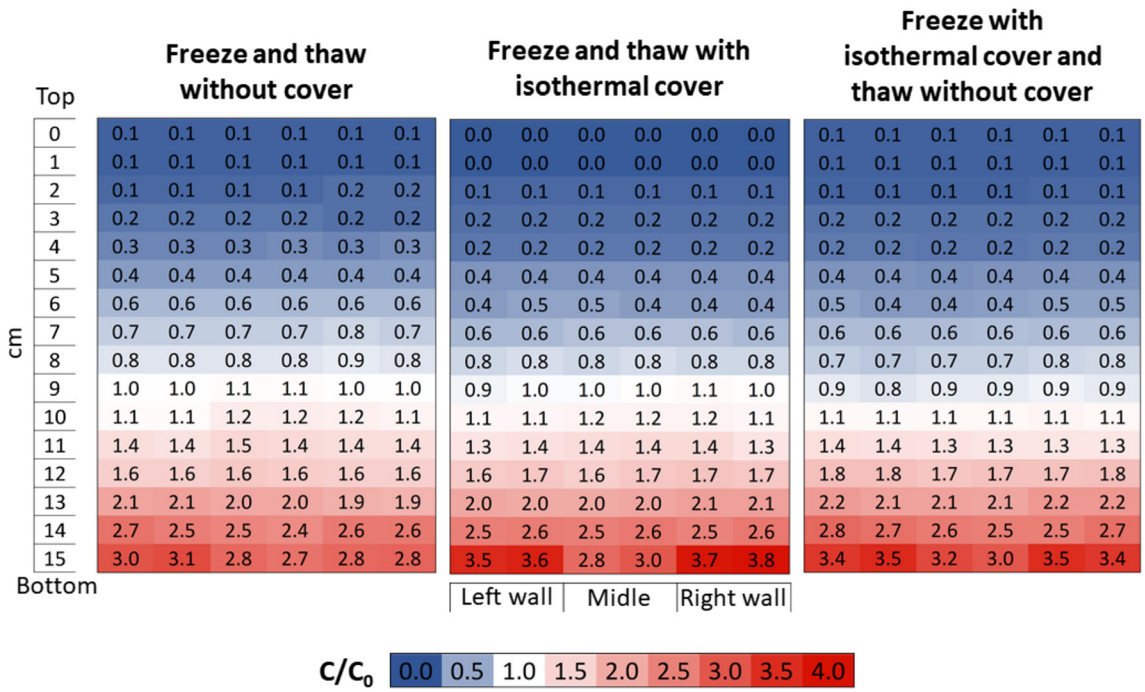

Fig. 11. Solute redistribution in a 2-L bottle after thawing at 6°C for 18 h. Three freeze–thaw assays were analyzed. A bottle frozen and thawed without a cover (left). A bottle frozen and thawed with an isothermal cover (middle). A bottle frozen with an isothermal cover and thawed without the cover (right). The samples were collected slowly and sequentially, in the center of the bottle and near the walls, from the top of the liquid surface to the bottom

layer of liquid being almost pure water, while in the bottom, the solutes were approximately 3 times more concentrated than the initial value.

DISCUSSION

The results presented herein expose the origin and nature of ice mounds that typically develop when biopharmaceutical formulations are frozen in bottles. The formation of an ice mound in the top of the bottles has been described in previous studies. Bezawada *et al.* (8) described this phenomenon as an upward volume expansion of the ice–liquid mixture that culminates in an "eruption" of highly concentrated liquid near the top of the liquid surface (similar to a volcanic eruption) when freezing a solution of azoalbumin with sucrose in a 125-mL bottle. However, to the best of our knowledge, mitigation strategies, such as the device we propose herein, have not been proposed as yet. This work shows that this adversity results from the faster freezing of the liquid at the top, at the air interface, enclosing a substantial portion of unfrozen solution (as shown in Figs. 5 and 6). The freezing of the enclosed solution generates pressure, forcing the liquid to percolate through the ice crust at the center, where the ice structure is more friable due to the higher temperature (compared with the ice near the walls). This work shows that internal pressure reached 10 bar in 5-L bottles, while 2-L bottles did not show significant pressure variation. Once the top freezes, hydrostatic pressure is released by the percolation of the liquid through the ice crust, thus forming a frozen mound; otherwise, pressure would rise much higher with the decrease of temperature, reaching values near 2 kbar (following water solid–liquid equilibrium) (10). Pressure is therefore expected to rise when the crust becomes thicker, or when the flow rate of liquid towards the top is higher, as for example, for bottles that have larger volume/interface ratio (such as 5 L compared with 2 L).

Three major factors are likely to contribute for the faster freezing of the liquid at the top: heat loss by radiation; heat loss through the convection of the air inside the bottle, which is exposed to significant temperature gradients; and also because constitutional supercooling is lower at the top. Constitutional supercooling is caused by the accumulation of solutes at the interface of growing ice crystals (depressing their growth). However, the concentrated liquid formed within the ice structure is denser and therefore more easily displaced from the top by natural convection (falls down), favoring crystal growth at this location (11,12). Heat loss by radiation and by convection of the internal air can be substantially mitigated by covering the bottle with insulation, because this attenuates the temperature gradients. However, the insulation cover was not enough to avoid the formation of an ice mound (Fig. 5b), showing that the ice growth is still significantly favored at the top. The ice crust was only prevented when a phase-change material (water) was used (isothermal cover). In this case, the heat released by the isothermal cover prevented ice from growing near the walls at the top of the liquid, *i.e.*, this subtle local heating was sufficient to enable a "V"-shaped freezing progression (Fig. 6). This strategy mitigated completely the formation of the ice mound, which can have multiple advantages for the cryopreservation of biological products. For example, this is expected to attenuate the percolation of the liquid phase (ice mounds are smaller), therefore preventing the raise of internal pressure, which can deform and/or rupture more fragile bottles, with a thinner polymer layer, brittle polymer materials, or larger volume/area ratio (bigger bottles) (Fig. 8).

Another important advance that results from preventing the ice crust is the release of bubbles, which have been correlated with higher protein aggregation rates and potentially acting as seeding interfaces for nucleation of protein aggregates (7,13–15). The MRI images show the internal air (bubble) spaces that are below the crust, forming a foam-like structure—as often described. This region has twice the volume in the uncovered bottles (Fig. 9). It is difficult to discriminate which phenomena, related to the formation of ice mounds, present higher threat to protein stability; however, the BSA aggregation mapping shown in Fig. 10 can provide evidence of critical aspects. Higher aggregation was observed in the uncovered bottle, with intense aggregation hotspots at the regions where bubbles are likely to be entrapped (as shown in Figs. 9 and 10). This correlates with the observation of Hauptmann *et al.* (7) that also found higher aggregation of monoclonal antibodies at the top of the bottles.

In general, no correlation is observed, in this work, between the cryoconcentration and the local fraction of BSA aggregates. Actually, concentrated regions appear to have lower intensity of aggregated species (center and bottom in Fig. 10). A similar observation was also reported by Hauptmann *et al.* (7) for monoclonal antibodies. However, the aggregation hotspots are more intense in the top "concentrated side" of the uncovered bottle. This is explained by the liquid-phase percolation inside the uncovered bottle, which pushes the concentrated liquid phase across the ice structure and through a path of least resistance, thus causing one side of the top (with higher ice porosity) to become more concentrated (as in Fig. 10), which also explains the layer of concentrated (percolated) phase that is present at the top (air interface) in the MRI (Fig. 9a). The higher interfacial stress, resulting from this pressure-driven flow through the ice structure, which is rich in entrapped bubbles (air interfaces), enhances protein aggregation, which could also be anticipated from previous reports (10,14–16). BSA was more sensitive to interfacial stress than to the concentration gradient, although this should not be generalized because high-concentration gradients have also been consistently reported as a risk factor (10,17).

The isothermal cover can act as a local cooler during thawing, which is not the design purpose. The effect of the cover on the overall stratification of the solutes during thawing is not significant; however, it tends to dilute further the top of the bottle (Fig. 11). Nonetheless, the results shown in Fig. 11 present a cautionary illustration for considering final homogenization of the solution (agitation) undergoing thawing, either with or without a cover.

CONCLUSION

The results presented herein explain the origin and nature of the ice mounds that form when biopharmaceutical formulations are frozen inside bottles. It was observed that the liquid freezes first at the top, forming an ice crust, which encloses the remaining unfrozen solution in the center of the bottle. As the enclosed liquid freezes, hydrostatic pressure rises, pushing the unfrozen solution through the ice crust towards the air interface, creating an ice mound. This effect exposes proteins to interfacial stresses and can also cause deformation of the containers.

The adverse effects of the ice crust were attenuated using an isothermal cover at the top of the bottle. The solution frozen in an uncovered bottle showed more aggregation, with higher intensity underneath the ice crust, where the bubbles were preeminent.

Overall, this work shows a correlation between ice mounds and protein interfacial stress caused by liquid percolation through ice and entrapped bubbles; it also presents a relatively simple mitigation strategy, which is the use of a top insulation with heating or a phase-change material.

ACKNOWLEDGMENTS

The authors would like to thank Cellon (Luxembourg) for providing the PharmaTainers.

FUNDING INFORMATION

This work was supported by the Portuguese national funds from Portugal 2020, Lisboa 2020, and European Union through Fundo Europeu do Desenvolvimento Regional (Project 17653, Cryocube).

COMPLIANCE WITH ETHICAL STANDARDS

Conflict of Interest SmartFreeZ has filed for intellectual property rights on devices related to the science reported in the manuscript.

REFERENCES

1. Kolhe P, Goswami S. Bulk protein solution: freeze–thaw process, storage and shipping considerations. In: Warne NW, Mahler H-C, editors. Challenges Protein Prod Dev. 1st ed: Springer International Publishing; 2018. p. 313–36.
2. Goldstein A, Pohlscheidt M, Loesch J, Mazzarella K, Bieger B, Lam P, *et al.* Disposable freeze systems in the pharmaceutical industry. Am Pharm Rev. 2012;15(7).
3. Singh SK, Kolhe P, Wang W, Nema S. Large-scale freezing of biologics-a practitioner's review. Part two: practical advice. Bioprocess Int. 2009;7:34–42.
4. Singh SK, Rathore N, McAuley A, Rathore AS. Best practices for the formulation and manufacturing of biotech drug products. BioPharm Int. 2009;22:32–48.
5. Kilburn D, Malliett A, Wong R. Evaluating single-use frozen storage systems. Am Pharm Rev. 2010;13:12–9.
6. Jameel F, Padala C, Randolph TW. Strategies for bulk storage and shipment of proteins. In: Jameel F, Hershenson S, editors. Formulation and process development strategies manufacturing biopharmaceuticals. Hoboken: John Wiley & Sons, Inc.; 2010. p. 677–704.
7. Hauptmann A, Hoelzl G, Loerting T. Distribution of protein content and number of aggregates in monoclonal antibody formulation after large-scale freezing. AAPS PharmSciTech. 2019;20:1–11.
8. Bezawada A, Thompson M, Cui W. Use of blast freezers in vaccine manufacture. Bioprocess Int. 2011;9:42–51.
9. Mahdjoub R, Chouvenc P, Seurin MJ, Andrieu J, Briguet A. Sucrose solution freezing studied by magnetic resonance imaging. Carbohydr Res. 2006;341:492–8.
10. Authelin J-R, Rodrigues MA, Tchessalov S, Singh SK, McCoy T, Wang S, *et al.* Freezing of biologicals revisited: scale, stability,

excipients, and degradation stresses. J Pharm Sci. 2020;109:44–61.
11. Rodrigues MA, Miller MA, Glass MA, Singh SK, Johnston KP. Effect of freezing rate and dendritic ice formation on concentration profiles of proteins frozen in cylindrical vessels. J Pharm Sci. 2011;100:1316–29.
12. Rodrigues MA, Balzan G, Rosa M, Gomes D, de Azevedo EG, Singh SK, *et al.* The importance of heat flow direction for reproducible and homogeneous freezing of bulk protein solutions. Biotechnol Prog. 2013;29:1212–21.
13. Miller R, Fainerman VB, Makievski AV, Krägel J, Grigoriev DO, Kazakov VN, *et al.* Dynamics of protein and mixed protein/surfactant adsorption layers at the water/fluid interface. Adv Colloid Interf Sci. 2000;89:39–82.
14. Gerhardt A, McGraw NR, Schwartz DK, Bee JS, Carpenter JF, Randolph TW. Protein aggregation and particle formation in prefilled glass syringes. J Pharm Sci. 2014;103:1601–12.
15. Xu Y, Grobelny P, Von Allmen A, Knudson K, Pikal M, Carpenter JF, *et al.* Protein quantity on the air-solid interface determines degradation rates of human growth hormone in lyophilized samples. J Pharm Sci. 2014;103:1356–66.
16. Varshney DB, Elliott JA, Gatlin LA, Kumar S, Suryanarayanan R, Shalaev EY. Synchrotron X-ray diffraction investigation of the anomalous behavior of ice during freezing of aqueous systems. J Phys Chem B. 2009;113:6177–82.
17. Mehta SB, Subramanian S, D'Mello R, Brisbane C, Roy S. Effect of protein cryoconcentration and processing conditions on kinetics of dimer formation for a monoclonal antibody: a case study on bioprocessing. Biotechnol Prog. 2019;35:1–7.